scientific reports

Check for updates

OPEN

# TRIM44 enhances autophagy via SQSTM1 oligomerization in response to oxidative stress

Yuqin Wang, Lin Lyu, Trung Vu & Nami McCarty✉

**The deubiquitinase tripartite motif containing 44 (TRIM44) plays a critical role in linking the proteotoxic stress response with autophagic degradation, which is significant in the context of cancer and neurological diseases. Although TRIM44 is recognized as a prognostic marker in various cancers, the complex molecular mechanisms through which it facilitates autophagic degradation, particularly under oxidative stress conditions, have not been fully explored. In this study, we demonstrate that TRIM44 significantly enhances autophagy in response to oxidative stress, reducing cytotoxicity in cancer cells treated with arsenic trioxide. Our research emphasizes the critical role of the posttranslational modification of sequestosome-1 (SQSTM1) and its importance in improving sequestration during autophagic degradation under oxidative stress. We found that TRIM44 notably promotes SQSTM1 oligomerization in both PB1 domain-dependent and oxidation-dependent manners. Furthermore, TRIM44 amplifies the interaction between protein kinase A and oligomerized SQSTM1, leading to enhanced phosphorylation of SQSTM1 at S349. This phosphorylation event activates NFE2L2, a key transcription factor in the oxidative stress response, highlighting the importance of TRIM44 in modulating SQSTM1-mediated autophagy. Our findings support that TRIM44 plays pivotal roles in regulating autophagic sensitivity to oxidative stress, with implications for cancer, aging, aging-associated diseases, and neurodegenerative disorders.**

Pathological processes such as cancer, aging, and age-related diseases, as well as neurodegenerative diseases, are commonly associated with oxidative damage to DNA and proteins[1–5]. Cellular homeostasis is maintained through a myriad of mechanisms, including autophagy, which functions to degrade damaged proteins and organelles that could be potentially toxic under basal conditions[6]. Furthermore, autophagy plays a pivotal role in ensuring cell survival under various stress conditions, including chemotherapy-induced oxidative stress[7]. Since the approval of arsenic trioxide (As[III]) as the frontline therapy for acute promyelocytic leukemia, its anticancer properties for various malignancies have been intensively investigated[8]. As[III] has proven effective not only in treating chronic lymphocytic leukemia and acute myeloid leukemia but also in some solid tumors such as cervical cancer, hepatocellular carcinoma, head and neck cancers, lung cancer, and stomach cancer[9]. Autophagy is activated in response to oxidative stress induced by As[III] to protect cells from apoptosis[10]. The KEAP1-NFE2L2 system is a well-established cellular defense mechanism against oxidative stress and electrophilic disturbances[11]. Modifications of KEAP1 cysteine residues result in its degradation, stabilizing NFE2L2, leading to its translocation to the nucleus, and subsequent transcriptional activation of cytoprotective genes through heterodimerization with small Maf proteins. Beyond this canonical pathway, SQSTM1, a recognized autophagic adaptor, binds to the NFE2L2-binding site on KEAP1, competitively inhibiting the KEAP1-NFE2L2 interaction, critical for the transcription of genes encoding antioxidant proteins and anti-inflammatory enzymes[12,13]. However, the pathogenic implications of KEAP1-NFE2L2 regulation by SQSTM1 and its connection with autophagic degradation are not fully clarified. Members of the TRIM family are involved in a spectrum of cellular functions, including regulation of the immune system, antiviral responses, autophagy-related receptor regulation, and cancer initiation[14]. Distinguishing itself within the TRIM family proteins, TRIM44 possesses a zinc finger ubiquitin protease domain (ZF-UBP) at its N terminus, functioning as a deubiquitinating enzyme, as opposed to the more common RING domain[15]. Since its initial discovery in 2001[16], TRIM44 has been found to be upregulated in multiple human tumors[17–20] and is associated with poor prognosis. However, the detailed molecular mechanisms of TRIM44's role in tumor initiation and/or progression remain elusive. Our previous research indicated that TRIM44 plays an important role in promoting autophagy by facilitating the oligomerization of SQSTM1 in 2001[21]. Therapeutically targeting

Brown Foundation Institute of Molecular Medicine for the Prevention of Human Diseases (IMM), The University of Texas-Health Science Center at Houston, 1825 Pressler St., IMM-630A, Houston, TX 77030, USA. ✉email: nami.mccarty@uth.tmc.edu

autophagy is showing promise in cancer patients[22]. However, the precise mechanism by which TRIM44 augments SQSTM1 oligomerization needs further elucidation.

In this study, we demonstrate that TRIM44 promotes the oligomerization of SQSTM1, dependent on its deubiquitinating activity. Moreover, the oligomerization of SQSTM1 mediated by TRIM44 is PB1 domain-dependent and oxidation-dependent. This TRIM44driven oligomerization fosters the phosphorylation of SQSTM1 at S349 via PKA signaling, leading to the sequestration of KEAP1 and subsequent activation of the NFE2L2-mediated antioxidant response. Thus, TRIM44 plays a substantial role in SQSTM1-mediated autophagy, protecting cells from oxidative stresses by enhancing the autophagic process.

## Results

### TRIM44 alleviates cytotoxicity via enhancing autophagy in response to oxidative stress

To investigate whether TRIM44 plays a key role in promoting cancer cell survival under oxidative stress induced by arsenic trioxide, we engineered cell lines with either upregulated (TRIM44[OE]) or downregulated TRIM44 (TRIM44[KD]) using a lentiviral system as full knockout proved lethal[23] (Supplementary Fig. S1A) and treated cells with arsenic trioxide. Cells overexpressing TRIM44 exhibited markedly increased resistance to As[III]-induced cytotoxicity compared to control cells. In contrast, TRIM44 knockdown resulted in reduced resistance to As[III] (Fig. 1A–C), underscoring TRIM44's potential role in cell survival upon exposure to oxidative stress.

Given that TRIM44 has recently been identified as a novel link connecting the UPS system with the autophagy degradation pathway[21] and it has been shown that autophagy is activated in response to oxidative stress to protect the cells from apoptosis, we assessed autophagy activity in TRIM44 [OE] and TRIM44[KD] cancer cells under oxidative stress. Following As[III] treatment, we observed a significant increase in LC3-II levels in TRIM44[OE] cells compared to control cells. However, these levels markedly decreased in TRIM44[KD] cells (Fig. 1D), showing TRIM44's important role in modulating the autophagy pathway following oxidative stress.

We also explored the impact of TRIM44-mediated autophagy in mitigating oxidative stress. The addition of 3-MA, an autophagy inhibitor, along with As[III] resulted in a notable increase in apoptosis. This effect was significantly distinct from that observed in individual treatments, indicating the critical role of TRIM44-induced autophagy in reducing apoptosis rates under oxidative stress (Fig. 1E). Collectively, our data supported that TRIM44 attenuates cytotoxicity via enhancing autophagy in response to oxidative stress.

### TRIM44 promotes the oligomerization of SQSTM1

TRIM44 is a three-domain protein consisting of an N-terminal zinc-finger UBP (ZF) with deubiquitinating activity, a b-box (BB) domain, and a coiled-coil domain (CC) (Fig. 2A), diverges from the typical E3 ligase function attributed to TRIM family members[24,25]. Our prior research pinpointed a critical role for TRIM44 in augmenting autophagy by facilitating SQSTM1 oligomerization[21]. To analyze the effect of TRIM44 on SQSTM1 oligomerization, we co-transfected Hela cells with HA-tagged SQSTM1 and the full-length (FL) form of TRIM44, as HeLa cells are the best model for studying SQSTM1 oligomerization in cancers[26,27]. Co-transfection experiments followed by immunofluorescence analysis, revealed a pronounced increase in SQSTM1 oligomerization, compared to the GFP control (Fig. 2B and C). Conversely, cells expressing a truncated TRIM44 lacking the ZF domain (TRIM44ΔZF) displayed a marked reduction in SQSTM1 oligomerization, underscoring the essential role of the ZF domain's deubiquitinating activity in mediating this process (Fig. 2B and C).

Under non-reducing conditions, monomeric SQSTM1 typically presents as a 62 kDa band, which shifts to higher molecular weight complexes upon oligomerization or protein interaction[28]. To further delineate TRIM44's effect on SQSTM1 oligomerization, we analyzed the SQSTM1 oligomerization in TRIM44[OE] cells. Overexpression of TRIM44 was found to enhance SQSTM1 oligomerization, whereas its knockdown reduced oligomerization following oxidative stress (Supplementary Fig. S1B). The ubiquitination of SQSTM1 hinders its dimerization and subsequent formation of oligomerization[28]. To explore this, we conducted a deubiquitylation assay using 293T cells, the most common cell line for analyzing the interaction between SQSTM1 and target proteins. We exogenously expressed SQSTM1 and TRIM44 in these cells.

We observed that TRIM44 expression decreased the level of ubiquitinated SQSTM1, while the inhibition of TRIM44 resulted in increased SQSTM1 ubiquitination (Supplementary Fig. S1C). Collectively, these findings support that TRIM44 deubiquitinating activity facilitates the oligomerization of SQSTM1.

To further elucidate the mechanism by which TRIM44 promotes the oligomerization of SQSTM1, we introduced mutations that disrupt oligomerization (D69A, K7R, or double mutation K7AD69A), which impeded dimerization and subsequent oligomer formation[26,28]. Remarkably, even with these mutations, oligomerization was significantly elevated in the presence of TRIM44, contrasting with GFP controls (Fig. 2D and E). Correspondingly, the reduced levels of ubiquitination from these mutations were confirmed (Fig. 2F, Supplementary Fig. S1D–G), aligning with previous studies[26,28]. We also introduced the Phox and Bem1p domain (PB1)—deleted form (ΔPB1) of SQSTM1, which is known to be required for self-oligomerization through interactions with other SQSTM1 molecules[29]. While deletion of the PB1 domain drastically reduced SQSTM1 oligomerization, TRIM44 still significantly boosted the oligomerization of this truncated form (Fig. 2G–I). Taken together, these data indicate that TRIM44 augments the oligomerization of SQSTM1 not only through the PB1 domain, highlighting TRIM44's significant influence on the oligomerization and subsequent functional modulation of SQSTM1.

### TRIM44 enhances SQSTM1 oligomerization in response to oxidative stresses

Oligomerization of SQSTM1 is facilitated by disulphide-linked conjugates (DLC) formation under oxidative stress conditions[30]. To investigate the alternative mechanism(s) of TRIM44-mediated oligomerization of SQSTM1, we exposed cultured cells to a range of treatments and analyzed them by immunofluorescence staining (Fig. 3A). We observed an increase in intracellular SQSTM1 aggregates in cells overexpressing TRIM44

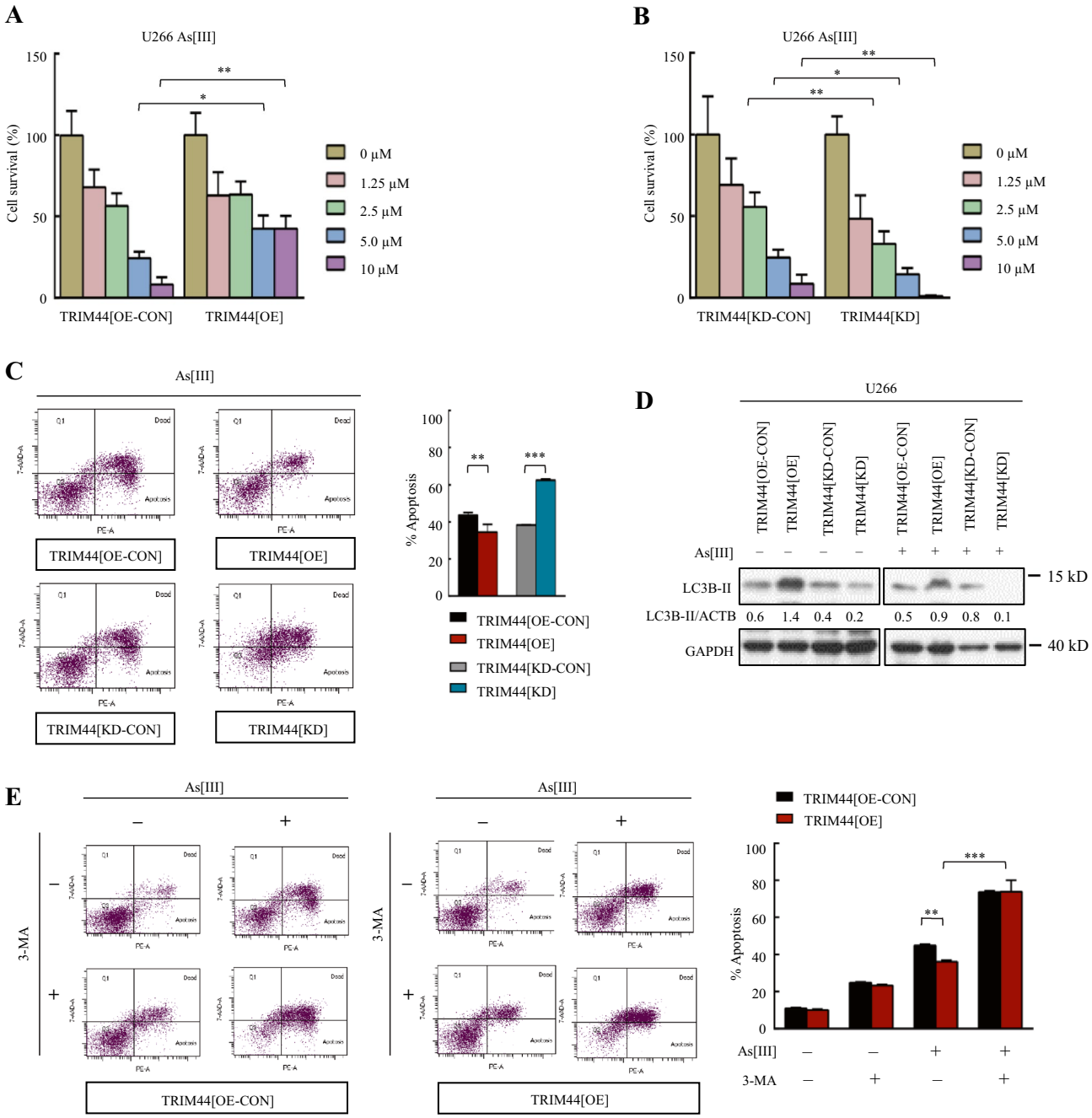


**Figure 1.** TRIM44 attenuates cytotoxicity via enhancing autophagy in response to oxidative stress. (**A**) Cell survival assay. U266 TRIM44[OE-CON] and TRIM44[OE] cells were challenged with different concentrations of As[III] as indicated for 24 h. Percentage of cell survival was determined by cell counting with trypan blue staining. Error bars represent s.e.m., n = 3, $^{*}P < 0.05$, $^{**}P < 0.01$ (unpaired *t*-tests). (**B**) Cell survival assay. U266 TRIM44[KD-CON] and TRIM44[KD] cells were challenged with different concentrations of As[III] as indicated for 24 h. Percentage of cell survival was determined by cell counting with trypan blue staining. Error bars represent s.e.m., n = 3, $^{*}P < 0.05$, $^{**}P < 0.01$ (unpaired *t*-tests). (**C**) Flow cytometry analysis. U266 cells were treated with or without As[III] (5 μM, 24 h) and then subjected to be stained with PE/7-AAD. Percentage of apoptosis was quantified. $^{**}P < 0.01$, $^{***}P < 0.001$ (unpaired *t*-tests). (**D**) Immunoblot analysis. U266 cells were treated with or without As[III] (5 μM) for 24 h. Cell lysates were then analyzed by immunoblotting for LC3B-II. GAPDH was used as a loading control. (**E**) Flow cytometry analysis. U266 cells were co-treated with or without As[III] (5 μM) and autophagy inhibitor 3-Methyladenine (3-MA, 500 μM) for 24 h. and then subjected to be stained with PE/7-AAD. Percentage of apoptosis was quantified. $^{**}P < 0.01$, $^{***}P < 0.001$ (unpaired *t*-tests).

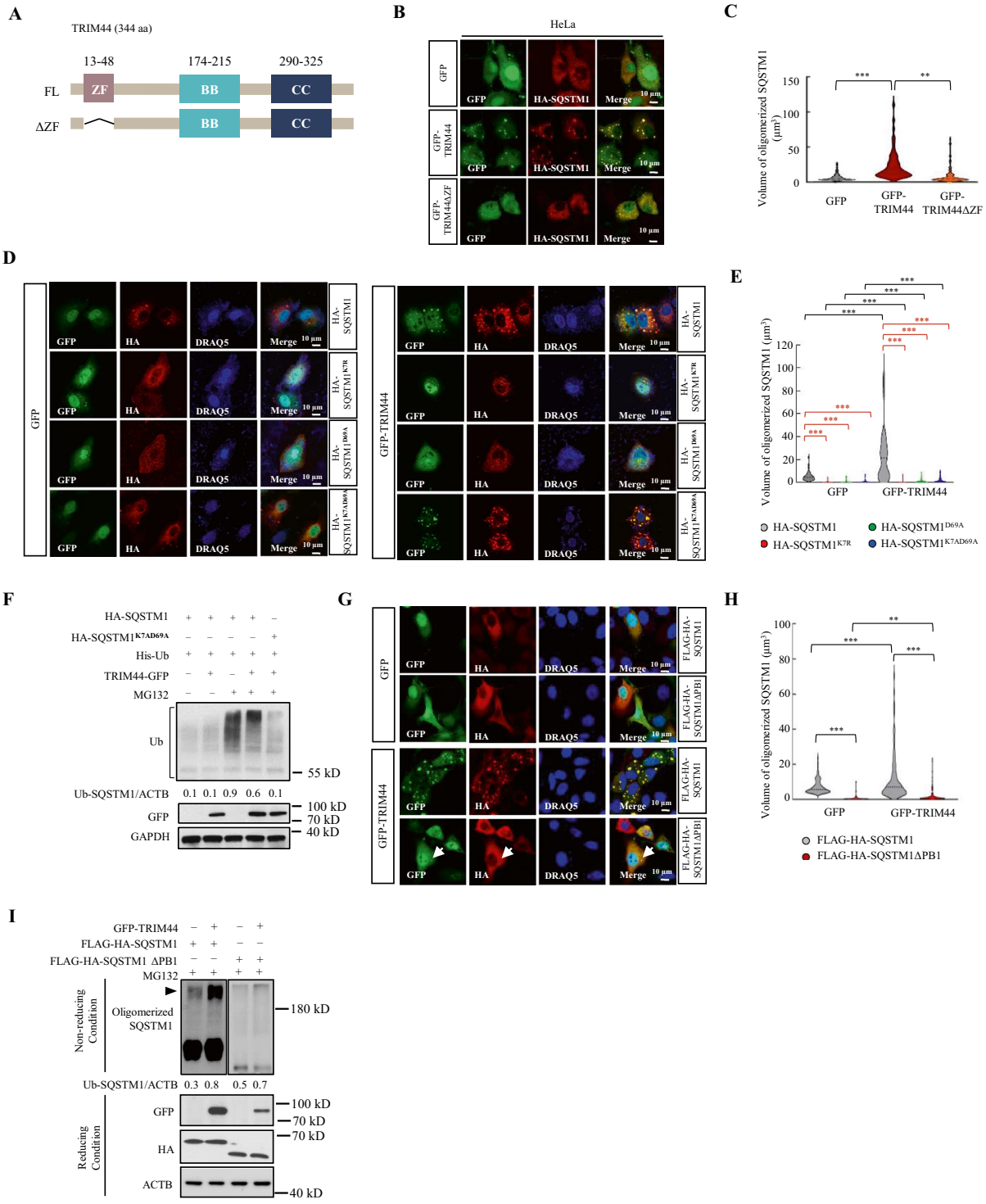


(TRIM44[OE]) compared to control cells (TRIM44[OE-CON]) without any treatment (Fig. 3A). The presence of autophagy inhibitors like Bafilomycin A1 (Baf A1), which blocks lysosomal acidification and degradation without affecting autophagosome-lysosome fusion[31], or Chloroquine (CQ), which affecting autophagosome-lysosome fusion, led to an intensified accumulation of SQSTM1 aggregates in TRIM44[OE] cells (Fig. 3A). This phenomenon was similarly observed under oxidative stress conditions induced by hydrogen peroxide ($H_2O_2$) or arsenic trioxide (As[III]), with TRIM44[OE] cells displaying a higher accumulation of SQSTM1 aggregates compared to TRIM44[OE-CON] cells (Fig. 3A). Conversely, the knockdown of TRIM44 resulted in a reduced formation of SQSTM1 aggregates under these treatments (Fig. 3A), implying that TRIM44 may be involved in the oligomerization promoting DLC formation in SQSTM1 under oxidative stresses. Additionally, we used rotenone, another oxidative stress inducer[32]. We observed a similar effect of TRIM44 on SQSTM1 aggregates following treatment with rotenone (Fig. S2A).

◂**Figure 2.** TRIM44 promotes SQSTM1 oligomerization. (**A**) The domain structure of TRIM44 protein. Depicts full-length (FL) TRIM44 (aa 1-344), ΔZF truncate (aa 48–344). (**B**) Confocal microscopy of HeLa cells co-transfected with HA-SQSTM1 and GFP, or GFP-TRIM44 full-length or GFP-TRIM44ΔZF. Immunostaining with HA antibody was done after 48 h. Scale bars represent 10 μm. (**C**) Graph illustrating the average volume of HA-SQSTM1 oligomerization. Average volume from 50 cells counted for each data point (bar). Statistical analysis via one-way ANOVA with Tukey's test, $^{**}P<0.01$, $^{***}P<0.001$. (**D**) Confocal microscopy of HeLa cells co-transfected with GFP or GFP-TRIM44 and specific HA-SQSTM1 constructs (HA-SQSTM1, HA-SQSTM1$^{K7R}$, HA-SQSTMQ$^{D69A}$, and HA-SQSTM1$^{K7AD69A}$). Immunostaining with HA antibody performed post 48 h. Scale bars: 10 μm. (**E**) Graph of average volume of HA-SQSTM1 constructs oligomerization (HA-SQSTM1, HA-SQSTM1$^{K7R}$, HA-SQSTM1$^{D69A}$, and HA-SQSTM1$^{K7AD69A}$). One-way ANOVA with Tukey's test for statistical analysis. $^{***}P<0.001$. Black star (*) denotes GFP-TRIM44 transfected cells versus corresponding GFP transfected cells. Red star (*) denotes HA-SQSTM1 mutants' transfected cells versus corresponding wild-type HA-SQSTM1 transfected cells. (**F**) In vivo deubiquitylation assay. 293T cells were co-transfected with HA-SQSTM1 constructs (HA-SQSTM1 and HA-SQSTM1$^{K7AD69A}$), His-Ubiquitin and GFP-TRIM44 plasmids. Post 48 h, cells were treated with proteasome inhibitor MG132 (5 μM, 6 h), followed by immunoprecipitation with HA antibody. Anti-Ub antibody was used to immunoblot ubiquitinated HA-SQSTM1 and HA-SQSTM1$^{K7AD69A}$. (**G**) HeLa cells were transfected with FLAG-HA-SQSTM1 or FLAG-HA-SQSTM1ΔPB1 mutant (lacking PB1 domain), in conjunction with either GFP or GFP-TRIM44. After 48 h, immunostaining was performed with HA (red) and DRAQ5 (blue). Scale bars represent 10 μm. (**H**) Graphic presentation of the average oligomerization volume of SQSTM1 (FLAG-HASQSTM1, FLAG-HA-SQSTM1ΔPB1). Each bar reflects the oligomerization volume of the indicated HA-SQSTM1 constructs in 50 cells. Statistical analysis was carried out using one-way ANOVA with Tukey's test, with $^{**}P<0.01$ and $^{***}P<0.001$. (**I**) 293T cells were co-transfected with the indicated plasmids. After 48 h, cells were cross-linked with DSP (0.4 mg/ml, 4 °C, 2 h) and processed under either reducing (with β-ME) or nonreducing conditions (without β-ME). The lysates were then subjected to immunoblotting using the indicated antibodies.

To further probe TRIM44's impact on the oligomerization of SQSTM1 primed by DLC formation, a DLC-formation deficient SQSTM1 mutation (C105/C113A) was employed in our immunofluorescence staining. The levels of oligomerization from this mutation were both markedly reduced in GFP-positive cells and GFP-TRIM44-positive cells, suggesting that DLC formation promotes SQSTM1 oligomerization and its affinity for ubiquitin-positive aggregates under oxidative stress, and the oligomerization of SQSTM1 mediated by TRIM44 is partly derived from DLC formation (Fig. 3B). The application of the reactive oxygen species (ROS) scavenger N-acetyl-l-cysteine (NAC) resulted in a decrease in SQSTM1 oligomerization levels, confirming the response of SQSTM1 oligomerization to oxidative stress (Fig. 3C–E). Moreover, GFP-TRIM44 positive cells showed a more pronounced reduction in SQSTM1 oligomerization when treated with NAC, indicating that TRIM44 enhances SQSTM1 oligomerization not solely via deubiquitinating activity but also by increasing intracellular ROS levels (Fig. 3C–E). Taken together, these findings point to TRIM44's capacity to modulate SQSTM1 oligomerization through both the PB1 domain and oxidation of SQSTM1.

## Oligomerization of SQSTM1 is essential for its phosphorylation

The capacity of SQSTM1 to adjust to redox shifts underpins its aggregation, particularly under oxidative stress—a mechanism crucial for vertebrate survival, providing defense during ageing[30]. Building on previous studies that identified phosphorylation sites on SQSTM1 at S349, S403, and S407, which are critical for substrate binding[33–35], we sought to explore the interplay between redox sensing-driven SQSTM1 oligomerization and its phosphorylation patterns. To this end, HeLa cells stably expressing either wild-type SQSTM1 or its oxidation-insensitive mutations (C105/113A, K102E) were treated with As[III] and analyzed by western blotting under non-reducing and reducing conditions. These two mutations exhibited a marked reduction in oligomerization, displaying a dose-dependent decline post-treatment, thereby underscoring the redox-sensitivity of SQSTM1 as a determinant of its oligomerization during oxidative stress (Fig. 4A).

Oligomerization of SQSTM1 precedes its sequential phosphorylations at serine residues (S407, S403), followed by phosphorylation at S349 within its UBA domain. The phosphorylation at S349 enhances SQSTM1's binding to KEAP1, leading to the release of NFE2L2 from KEAP1 and subsequent activation of NFE2L2's targets involved in antioxidant and anti-inflammation processes[33,36]. Our data showed that hindered SQSTM1 oligomerization led to attenuated phosphorylation at S349 (Fig. 4B and C). On the other side, the phosphorylation-deficient mutation SQSTM1 S349A did not prevent SQSTM1 oligomerization (Fig. 4D and E), supporting that SQSTM1 oligomerization is a prerequisite for the phosphorylation of SQSTM1 S349.

## TRIM44 enhances phosphorylation of SQSTM1 at S349 via PKA

Given that TRIM44 promotes SQSTM1 oligomerization, and SQSTM1 oligomerization is required for its phosphorylation, we delved into the mechanism by which TRIM44 regulates the phosphorylation of SQSTM1 at S349. Enhanced phosphorylation at this site was observed in cells with TRIM44 overexpression (TRIM44[OE]), while a reduction was noted upon TRIM44 knockdown (TRIM44[KD]) (Supplementary Fig. S3A and B). When challenged with As[III], TRIM44[OE] cells exhibited a pronounced increase in SQSTM1 S349 phosphorylation compared to the control group (TRIM44[OE-CON]) (Fig. 4C).

The kinase responsible for phosphorylating SQSTM1 at S349 has been a subject of debate. Although the involvement of the mammalian target of rapamycin (mTOR) in the phosphorylation at this site has been reported[33], our data indicated that suppression of mTOR activity by an inhibitor pp242 (mTORi), did not abolish

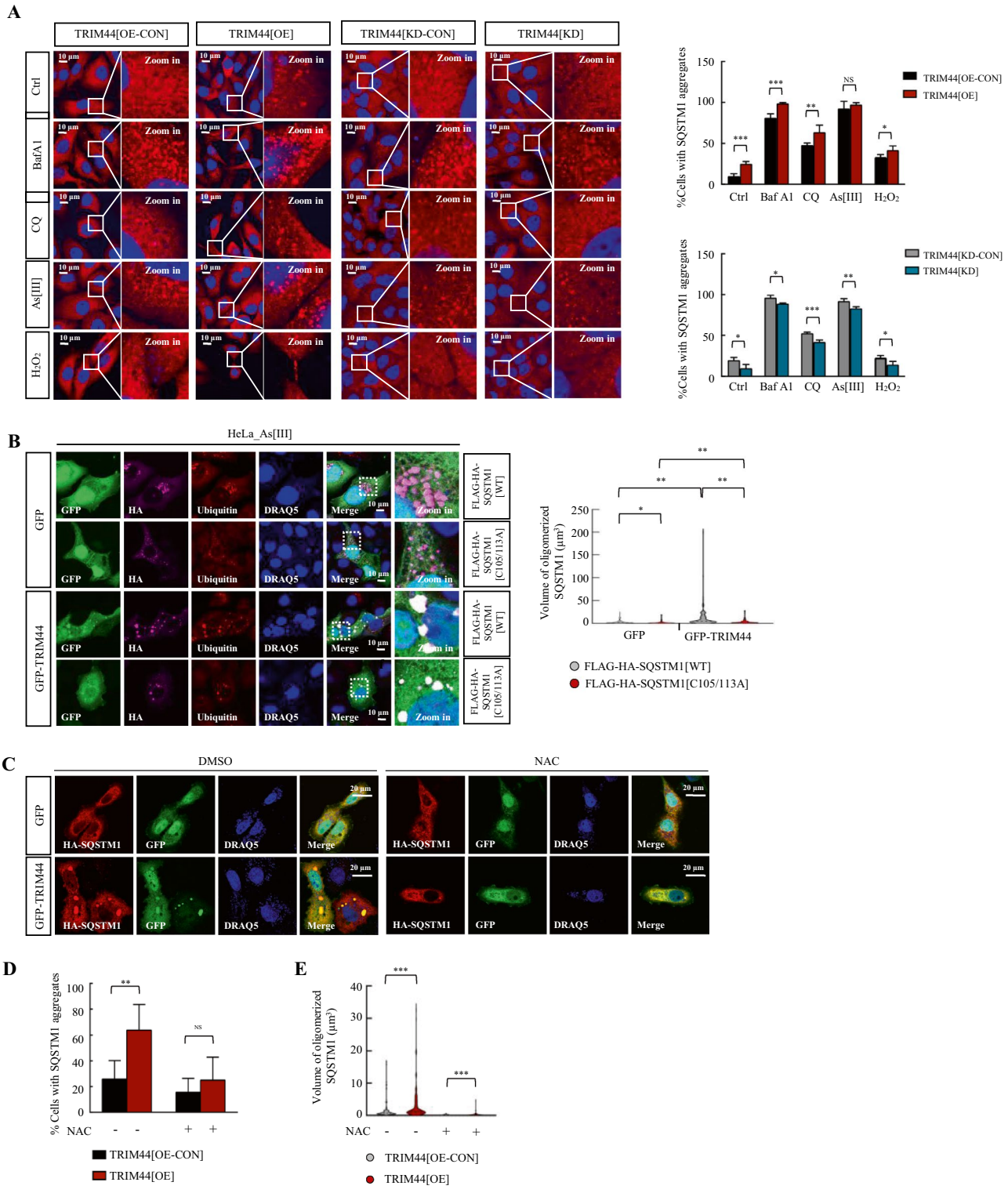


**Figure 3.** TRIM44 promotes SQSTM1 oligomerization in response to oxidative stresses. (**A**) Confocal microscopy of HeLa stable cells (TRIM44[OE-CON], or TRIM44[OE], TRIM44[KD-CON] and TRIM44[KD]) treated with Bafilomycin A1 (Baf A1, 400 nM, 4 h), or chloroquine (CQ, 50 μM, 4 h), or arsenic trioxide (As[III], 5 μM, 4 h), or hydrogen peroxide ($H_2O_2$, 3 mM, 10 min). Immunostaining with anti-SQSTM1 antibody was performed. Cells with more than two visible SQSTM1 aggregates were considered positive. n = 3, mean ± SD, $^*P < 0.05$, $^{**}P < 0.01$, $^{***}P < 0.005$ (Student's unpaired *t* test). (**B**) Immunofluorescence staining of HeLa cells co-transfected with indicated plasmids. After 48 h, cells were challenged with As[III] (5 μM, 24 h) and immunostained with anti-HA (magenta), anti-ubiquitin (red), and DRAQ5 (blue). Volume of oligomerized SQSTM1 was quantified (mean ± SD, n = 3, $^{**}P < 0.01$, $^{***}P < 0.005$, one-way ANOVA with Tukey's test). (**C**) Immunofluorescence staining. HeLa cells co-transfected with indicated plasmids. After 24 h, cells were treated with or without NAC (0.2 mM, 24 h). Immunostaining with anti-HA antibody (red) and DRAQ5 (blue) was performed. Scale bars represent 20 μm. (**D**) Percentage of cells with SQSTM1 aggregates was quantified. Cells with more than two visible SQSTM1 aggregates were considered positive (n = 3, mean ± SD, $^{**}P < 0.01$ (Student's unpaired *t* test). (**E**) Volume of oligomerized SQSTM1 was quantified. Student's unpaired *t* test was used for statistical analysis ($^{***}P < 0.001$).

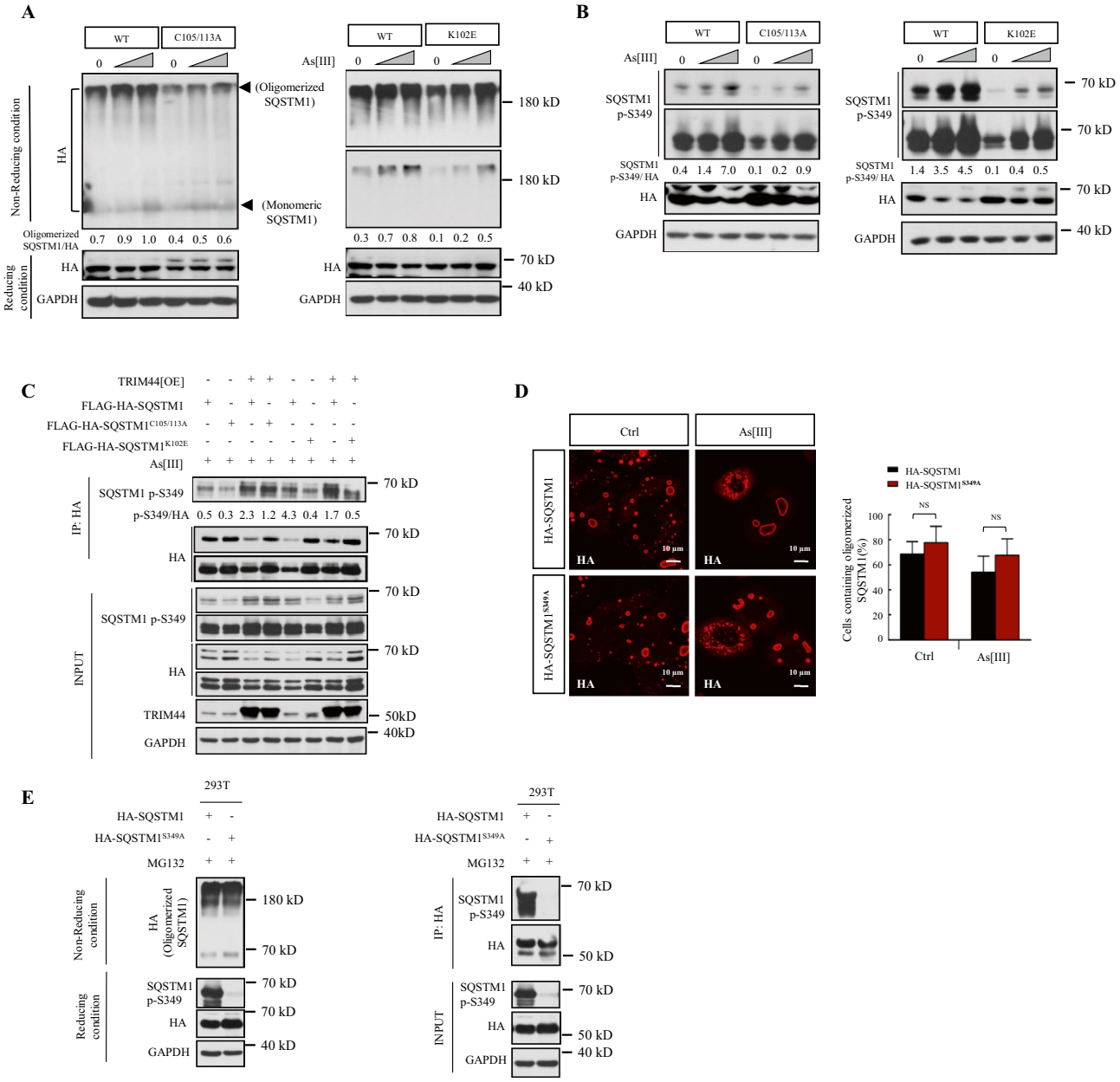


**Figure 4.** Oligomerization of SQSTM1 is essential for its phosphorylation at S349. (**A**) HeLa cells stable expressing WT FLAG-HA-SQSTM1 (WT), FLAG-HA-SQSTM1 [C105/113A] (C105/113A) or FLAG-HA-SQSTM1[K102E] (K102E) were treated with As[III] (from 2.5 to 5 µM, 6 h), followed by cross-linking with DSP (0.4 mg/ml, 4 °C, 2 h). Cell lysates, prepared under reducing (with β-ME) or non-reducing condition (without β-ME), were subjected to immunoblotting for indicated antibodies. (**B**) 293T cells stably expressing WT FLAG-HA-SQSTM1, FLAG-HA SQSTM1[C105/113A] (C105/113A) or FLAG-HA-SQSTM1[K102E] (K102E) were treated with As[III] (from 2.5 to 5 µM, 6 h). Whole-cell lysates were examined for SQSTM1 p-S349, HA expression by immunoblotting (GAPDH was used as a loading control). (**C**) 293T cells stably co-expressing indicated SQSTM1 wild-type or SQSTM1 mutations with or without TRIM44 were treated with As[III] (5 µM) for 6 h. Immunoprecipation was performed with anti-HA antibody and immunoblotting for SQSTM1 p-S349 and HA. (**D**) Immunofluorescence staining of HeLa cells transfected with indicated HA-SQSTM1 constructs (HA-SQSTM1, and HA-SQSTM1$^{S349A}$). After 48 h, cells were treated with or without As[III] (5 µM, 24 h). Immunostaining with anti-HA antibody was performed. Percentage of cells containing oligomerized SQSTM1 was analyzed. Cells with more than two visible SQSTM1 aggregates were considered positive. n = 3, mean ± SD. NS, non-significant (Student's unpaired *t test*). (**E**) 293T cells were transfected with HA-SQSTM1 constructs and expressed to MG132 (5 µM) for a duration of 6 h. The treated cells were subsequently cross-linked with DSP (0.4 mg/ml, 4 °C, 2 h) and prepared under either reducing conditions (with β-ME) or nonreducing condition (without β-ME). Cell lysates were subjected to immunoblotting for the indicated antibodies. Immunoprecipitation was executed using an anti-HA antibody and immunoblotting for SQSTM1 p-S349 and HA.

TRIM44's enhancement of SQSTM1 phosphorylation under either basal or oxidative conditions (Supplementary Fig. S2D and F). This holds true even though TRIM44[OE] cells exhibited suppressed mTOR activity (Supplementary Fig. S3C).

A previous study identified initial phosphorylation of serine 407 in SQSTM1's UBA domain by the Unc-51-like autophagy activating kinase 1 (ULK1). Subsequent phosphorylation at serine 403 by either casein kinase 2 (CK2), TANK-binding kinase 1 (TBK1), or ULK1 enhances SQSTM1's binding affinity for ubiquitin-chains[36]. On this basis, we investigated whether TRIM44 influences SQSTM1's pS349 via these kinases. Our results confirmed that inhibiting these kinases did not alter the TRIM44-mediated increase in SQSTM1 pS349 levels in TRIM44[OE] cells (Supplementary Fig. S3D). Also, we did not see any increased level of these kinases in TRIM44[OE] cells and decreased levels of these kinases in TRIM44[KD] cells (Supplementary Fig. S3E).

To further investigate into the mechanism behind TRIM44-mediated phosphorylation of SQSTM1 at S349, NetPhos was initially employed to predict the potential kinase targeting SQSTM1 S349. Additionally, kinases interacting with TRIM44 were screened from our mass spectrometry data (unpublished). From these findings, we focused on four candidates glycogen synthase kinase 3 (GSK3), $Ca^{2+}$/calmodulin dependent protein kinase II (CaM-II), protein kinase A (PKA) and casein kinase 1 (CKI). Screening with inhibitors specific to these kinases in TRIM44[OE] cells revealed that only inhibition of PKA suppressed the TRIM44-induced phosphorylation at S349, while inhibitors of GSK3, CaM-II, and CKI had no significant effect (Fig. 5A and Supplementary Fig. S3G). This was corroborated by a significant increase in PKA activity in TRIM44[OE] cells and a decrease in TRIM44[KD] cells (Fig. 5B), with a notable increase in SQSTM1 pS349 in the anti-phospho-PKA substrate fraction, particularly under oxidative stress (Fig. 5C).

Next, we examined whether PKA catalytic subunit α (PKA Cα) expression might be altered by TRIM44. As shown in Fig. 5D, PKA Cα was reduced in TRIM44[KD] cells under basal and oxidative stress conditions. We further validated the involvement of PKA in TRIM44-mediated SQSTM1 S349 phosphorylation using siRNA transfection. Silencing PKA Cα resulted in a marked reduction in this phosphorylation in TRIM44[OE] cells (Fig. 5E). Conversely, overexpressing PKA Cα in TRIM44[KD] cells restored phosphorylation levels (Supplementary Fig. S3H). Consistent with this, we observed that the interaction between PKA Cα and SQSTM1 was enhanced in TRIM44[OE] cells and a further increase following Bafilomycin A1 (Baf A1) treatment (Fig. 5F). In addition, the affinity of PKA Cα and SQSTM1 was abolished by oligomerization-deficient mutation K7R, supporting that TRIM44 promotes SQSTM1 S349 phosphorylation by enhancing the interaction between PKA and oligomerized SQSTM1 (Supplementary Fig. S3I). These findings collectively highlight that TRIM44-mediated SQSTM1 phosphorylation at S349 is achieved by upregulating PKA Cα-induced PKA signaling.

## TRIM44-induced SQSTM1 oligomerization promotes KEAP1 sequestration and potentiates NFE2L2 activation

KEAP1 is a substrate of autophagy, and the interaction of KEAP1 with SQSTM1 is indispensable for its autophagic degradation[37]. Phosphorylation of SQSTM1 at serine 349 enhances the interaction between SQSTM1 with KEAP1[38]. This observation introduces the concept that TRIM44 could augment the binding between SQSTM1 and KEAP1 and subsequent degradation of KEAP1. To address this, we initially evaluated TRIM44's influence on KEAP1 protein levels. Our data revealed that TRIM44 overexpression led to a decline in KEAP1 protein abundance, while suppression of TRIM44 resulted in an increase in KEAP1 (Fig. 6A and supplementary Fig. S4A).

Further investigation into KEAP1 degradation involved treating cells (TRIM44[OE-CON], TRIM44[OE], TRIM44[KD-CON], and TRIM44[KD]) with CHX, which inhibits new proteins synthesis. This is a useful tool for monitoring protein stability without the influence of newly synthesized proteins[39]. After eight hours, TRIM44[OE] cells demonstrated a marked reduction in KEAP1 levels compared to the TRIM44[OE-CON] group, an effect reversed by TRIM44 downregulation (Fig. 6B and Supplementary Fig. S4B).

Immunofluorescence analyses illuminated that cells with GFP-TRIM44 overexpression exhibited cytosolic FLAG-KEAP1 aggregating in conjunction with S349-phosphorylated SQSTM1, particularly post-As[III] exposure (Fig. 6C). Parallel to this, a higher accumulation of S349-phosphorylated SQSTM1 and KEAP1 in the detergent insoluble fraction was observed in TRIM44[OE] cells compared to TRIM44[OE-CON] cells (Fig. 6D). Moreover, TRIM44 significantly enhanced KEAP1 sequestration by SQSTM1 (Supplementary Fig. S4C and D), a process diminished with TRIM44 knockdown (Fig. 6E). This facilitatory role of TRIM44 in KEAP1 sequestration is dependent on SQSTM1, as silencing SQSTM1 eliminated KEAP1 sequestration in cells with high levels of TRIM44 (Supplementary Fig. S4E). Furthermore, TRIM44 was shown to potentiate the colocalization of KEAP1 and SQSTM1 with LC3B, an autophagy associated marker (Fig. 6F, Supplementary Fig. S4F). These results suggested that TRIM44 fosters sequestration of KEAP1 by SQSTM1. Additionally, immunoprecipitation results showed that KEAP1 had a higher affinity for oligomerized SQSTM1 (Fig. 6G), implying that TRIM44 promotes KEAP1 degradation by enhancing SQSTM1 oligomerization.

The KEAP1-NFE2L2 pathway is pivotal in the cellular defense against oxidative stress. NFE2L2, as a transcription factor, orchestrates the cellular adaptation to oxidative and electrophilic stress by activating antioxidant genes in response to redox imbalances[40]. Under stress conditions, KEAP1 is degraded and leads to the stabilization of NFE2L2, thereby allowing its accumulation and nuclear translocation to initiate the antioxidant transcriptional program[41]. Based on our findings that TRIM44 mediates KEAP1 degradation, we hypothesized that TRIM44 enhances NFE2L2 activity. Consistent with this hypothesis, TRIM44 overexpression correlated with elevated nuclear NFE2L2 level, while TRIM44 silencing reduced these levels, especially following As[III] exposure. This modulation in NFE2L2 localization was inversely related to cytoplasmic KEAP1 levels (Fig. 7A). Furthermore, a concomitant increase in the expression of NFE2L2 target genes, such as the heme oxygenase-1 (*HMOX1*) gene and thioredoxin (*TXN*), was observed both with or without As[III] treatment (Fig. 7B). Interestingly, the upregulation of NFE2L2 target genes occurred independently of changes in *NFE2L2* mRNA expression, with a

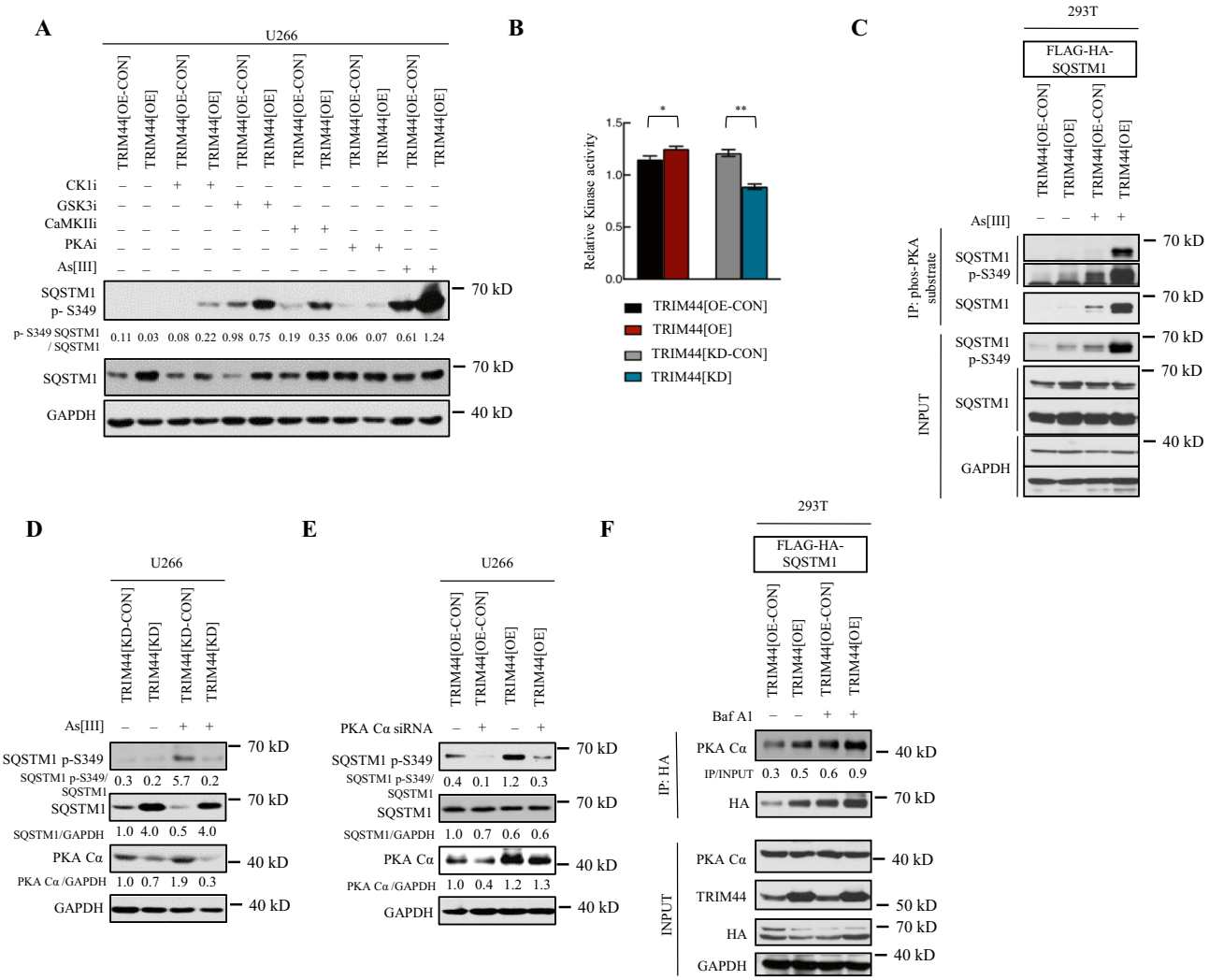


**Figure 5.** TRIM44 facilitates SQSTM1 S349 phosphorylation via PKA. (**A**) U266 TRIM44[OE-CON], TRIM44[OE] cells were exposed to inhibitors targeting CKI (CKI-7, 100 μM, 6 h), GSK3 (CHIR-99021, 2 μM, 24 h), CaMKII (KN-62, 1 μM, 24 h), and PKA (H89, 5 μM, 24 h), and As[III] (5 μM, 6 h) or left untreated. Whole-cell lysates were examined using anti-SQSTM1, anti-SQSTM1 p-S349. GAPDH served as a loading control. (**B**) Cell extracts from U266 TRIM44[OE-CON], TRIM44[OE], TRIM44[KD-CON] and TRIM44[KD] cells were lysed for measure PKA activity (PKA Kinase activity Kit, Abcam, ab139435). Measurements were made in triplicates, mean ± SD. Student's *t* test was used for statistical analysis $^{*}P < 0.05$, $^{**}P < 0.01$. (**C**) 293T cells stably co-expressing FLAG-HA-SQSTM1 with TRIM44 (TRIM44[OE]) or without TRIM44 (TRIM44[OE-CON) were treated with or without As[III] (5 μM, 6 h). Immunoprecipitation was subsequently performed with an anti-PKA substrate antibody and immunoblotting for indicated signals. (**D**) U266 TRIM44[KD-CON], TRIM44[KD] cells were treated with or without As[III] (5 μM, 24 h). Whole-cell lysates were analyzed via immunoblotting for SQSTM1 p-S349, SQSTM1, PKA Cα. (**E**) U266 TRIM44[OE-CON] and TRIM44[OE] cells were transfected with NC or PKA Cα siRNA. After 48 h, whole-cell lysates were analyzed via immunoblotting for SQSTM1 pS349 and SQSTM1, PKA Cα. (**F**) 293T cells stably co-expressing FLAG-HA-SQSTM1 with TRIM44 (TRIM44[OE]) or without TRIM44 (TRIM44[OE-CON) were treated with or without Baf A1 (100 nM, 6 h). Immunoprecipitation was subsequently performed with an anti-HA antibody and immunoblotting for indicated signals.

pronounced response to As[III] exposure (Fig. 7B, Supplementary Fig. S4G). However, this response was attenuated in TRIM44 knock-down cells (Fig. 7B).

To further validate TRIM44's impact on the KEAP1-NFE2L2 axis, immunoprecipitation assays were performed to examine the interaction between KEAP1 and SQSTM1, as well as the interaction between KEAP1 and NFE2L2 in 293T cells.

Our results revealed that an enhanced interaction between KEAP1 and SQSTM1 was observed in TRIM44[OE] cells, compared to control (TRIM44[OE-CON) (Fig. 7C), while the binding between KEAP1 and NFE2L2 was reduced in TRIM44[KD] cells (Fig. 7C). Aligning with these phenomena, TRIM44 disrupted the interaction between NFE2L2 and SQSTM1 (Fig. 7D).

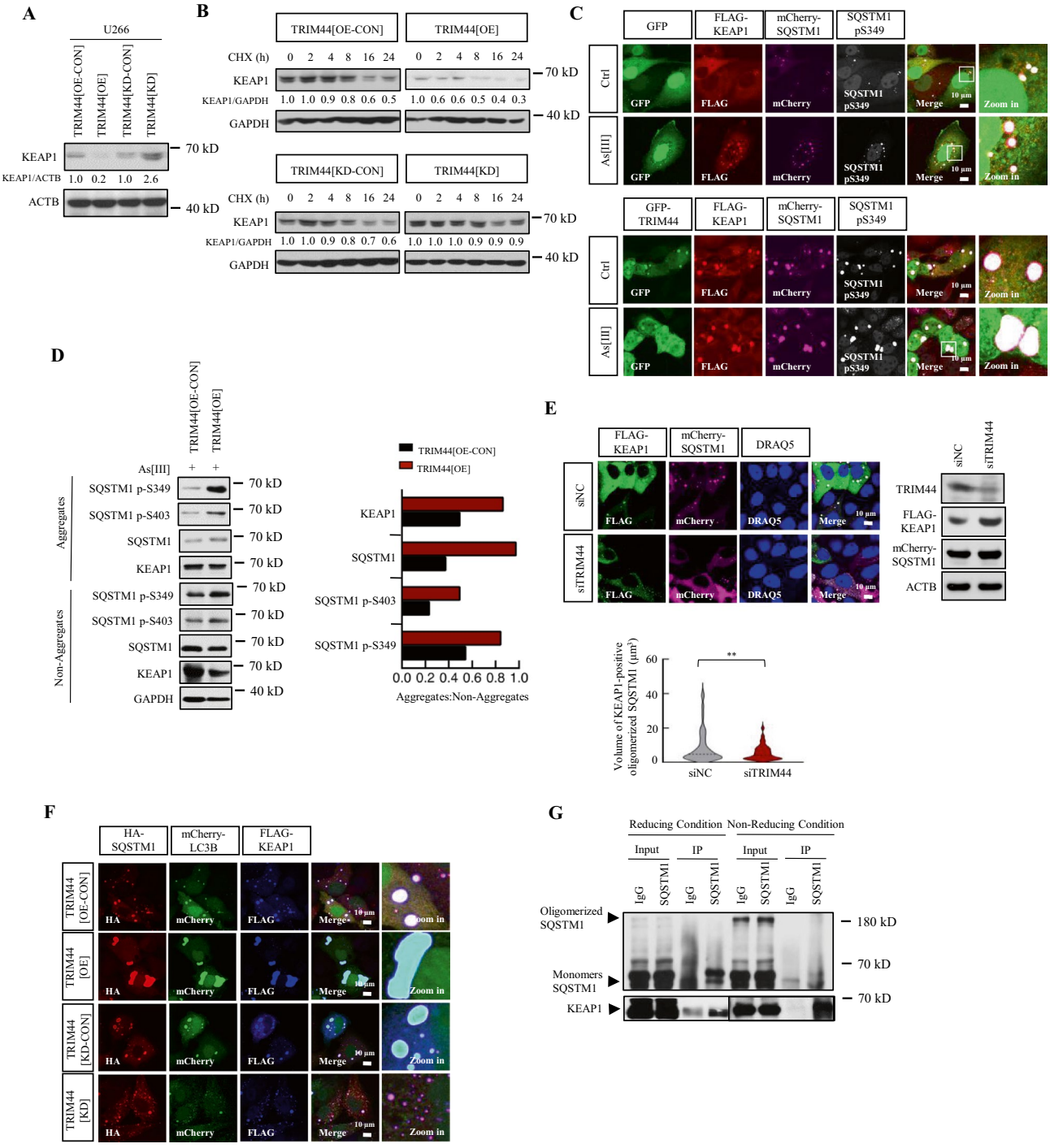


In vertebrates, SQSTM1's redox sensitivity plays a pivotal role in modulating autophagic degradation and cell survival under oxidative stresses[30]. Next we explored the effect of TRIM44 on the KEAP1-NFE2L2 pathway in the context of SQSTM1 redox-sensitivity-deficient mutation (C105/113A). In the context of wild-type SQSTM1 (WT), following oxidative stress, nuclear NFE2L2 was significantly increased in TRIM44[OE] cells, although considerable nuclear NFE2L2 was detected in TRIM44[OE-CON] cells. On the other hand, in the context of mutation SQSTM1 (C105/113A), following oxidative stress, almost no nuclear NFE2L2 was detected in TRIM44[OE-CON] cells. However, an increase of NFE2L2 level in nuclear fraction was observed in TRIM44[OE] cells (Fig. 7E).

We also investigated the role of PKA-mediated SQSTM1 oligomerization in NFE2L2 activation by TRIM44. The notable increase in NFE2L2 target gene expression mediated by TRIM44 was significantly suppressed following PKA Cα knockdown (Supplementary Fig. S5A and B). Conversely, overexpression of PKA Cα rescued the reduction in NFE2L2 target expression caused by TRIM44 silencing (Supplementary Fig. S5C). These findings support that PKA is involved in the TRIM44-driven cytoprotective activity of NFE2L2. Corroborating our findings, neither the mTOR inhibitor pp242 nor any other tested inhibitors affected the TRIM44-mediated NFE2L2

◂**Figure 6.** TRIM44-mediated phosphorylation of SQSTM1 accelerates KEAP1 degradation. (**A**) Immunoblot analysis was conducted on whole-cell lysates from U266 TRIM44[OECON], TRIM44[OE], TRIM44[KD-CON] and TRIM44[KD] cells, examining for KEAP1. (**B**) HeLa TRIM44[OE-CON], TRIM44[OE], TRIM44[KD-CON] and TRIM44[KD] cells were treated with cycloheximide (100 μg/ml) for specified durations. Whole-cell lysates were then analyzed via immunoblotting for KEAP1. GAPDH was utilized as a loading control. (**C**) Confocal microscopy of HeLa cells tri-transfected with FLAG-KEAP1, mCherry-SQSTM1 and GFP or GFP-TRIM44. After 24 h, cells were treated with or without As[III] for another 24 h. Immunostaining with anti-FLAG (red), and anti-SQSTM1 p-S349 (white) was performed. Expression of GFP-TRIM44 or GFP was shown as green, and mCherry-SQSTM1 was shown as magenta color. Scale bars represent 10 μm. (**D**) HeLa TRIM44[OE-CON] and TRIM44[OE] cells were treated with As[III] (5 μM) for 6 h. Whole-cell lysates were analyzed by immunoblotting. Non-Aggregates: NP-40-soluble; Aggregates: SDS-soluble, NP40 insoluble. Relative ratios of Non-Aggregates or Aggregates versus GAPDH are indicated. (**E**) HeLa cells were transfected with NC or TRIM44 siRNA. After 24 h, cells were then co-transfected with FLAG-KEAP1 and mCherry-SQSTM1 for another 24 h. Immunostaining with anti-FLAG antibody (green) and DRAQ5 (blue) were performed. Expression of mCherry-SQSTM1 was shown as magenta color. Scale bars represent 20 μm. Cells were also analyzed by immunoblotting for TRIM44, FLAG and mCherry. GAPDH was used as a loading control. Volume of KEAP1-positive oligomerized SQSTM1 was quantified. Student's unpaired *t* test was used for statistical analysis. $^{**}P < 0.01$. (**F**) Immunofluorescence staining. HeLa TRIM44[OE-CON], TRIM44[OE], TRIM44[KD-CON], TRIM44[KD] cells were tri-transfected with HA-SQSTM1, mCherry-LC3B, and FLAG-KEAP1. After 48 h, cells were immunostained with anti-HA (red), and anti-FLAG (blue). Expression of mCherry-LC3 was shown as green color. Scale bars, represent 10 μm. (**G**) 293T cells were co-transfected with FLAG-KEAP1 and mCherry-SQSTM1. After 48 h, the cells were treated with MG132 (5 μM, 6 h) and then treated with the crosslinking agent DSP (0.4 mg/ml, 4 °C) for 2 h. Subsequently, the cells were lysed in IP lysis buffer containing 1% SDS. The lysates were mixed with loading buffer containing β-ME for reducing condition or without β-ME (non-reducing condition). The samples were then subjected to SDS-PAGE and immunoblotting for SQSTM1 and KEAP1.

target upregulation (Supplementary Fig. S4H). In conclusion, our data support that TRIM44 plays a critical role in facilitating the oligomerization of SQSTM1 through interactions with PKA. This interaction serves as a key mechanism in enhancing the cytoprotective activity of NFE2L2, underscoring the significance of TRIM44 in cellular stress response pathways.

## Discussion

Oligomerization of SQSTM1 is essential for its targeting to autophagosome formation site and its subsequent sequestration function during autophagic degradation[28,42]. So far, two mechanisms have been reported for the formation of SQSTM1 oligomerization. One mechanism is PB1 domain-dependent, which is a non-covalent interaction formed by the hydrogen bond between K7 and D69[28,43,44]. The other mechanism is oxidation-dependent, which is a covalent interaction formed by intermolecular disulphide bond between oxidation-sensitive Cys residues[30].

Additionally, these two processes induce oligomerization independently. We identified TRIM44 promotes the oligomerization of SQSTM1 by enhancing these two interactions. As demonstrated in Fig. 4C, TRIM44 promotes the phosphorylation of two oxidationdeficient SQSTM1 mutations, indicating that TRIM44 increases the sensitivity of SQSTM1-mediated autophagy, especially under oxidative stresses.

The phosphorylation of SQSTM1 at S349 is pivotal for KEAP1 binding. However, the kinase(s) responsible for this site have been unclear. The first candidate kinase for this site is mTORC1. Inhibition of mTORC1 using rapamycin in mouse embryonic fibroblasts suppressed the phosphorylation of SQSTM1 at S349, as well as the expression levels of NFE2L2 targets[34]. Another potential kinase is ULK1, which is recently reported[45], although knockout of *Ulk1* and/or *Ulk2* had no effect on this phosphorylation following oxidative stress[34]. In our study, we did not observe any effect on the phosphorylation mediated by TRIM44 following inhibition of mTORC1 or ULK1 under basal and oxidative conditions (Supplementary Fig. S3D and F). Our findings reveal that a novel kinase PKA is responsible for the increased phosphorylation of SQSTM1 at S349 triggered by TRIM44.

In this study, we demonstrate that TRIM44 promotes SQSTM1 oligomerization via its deubiquitinating activity. The oligomerization primed by TRIM44 is not only PB1 domain-dependent but also oxidation-dependent. Furthermore, the oligomerization of SQSTM1 is essential for its phosphorylation at S349. PKA is responsible for the increased phosphorylation of SQSTM1 at S349 triggered by TRIM44, leading to more KEAP1 sequestration and then its degradation and subsequent activation of NFE2L2 under oxidative stress. This implies that TRIM44 might increase the sensitivity of SQSTM1-mediated autophagy under basal and oxidative conditions in cancer, ageing, ageing-associated diseases, and neurodegenerative diseases.

Importantly, this study also emphasized the role of TRIM44 in the regulation of autophagy in response to oxidative stress induced by As[III]. Although the clinical successes of As[III] in treating hematological cancers have not been translated to solid cancers due to the quick removal of As[III] by the body's immune system, immense progress has been made in delivering As[III] compounds specifically to cancer cells. Along with other arsenic compounds, As[III] has successfully been encapsulated in liposomes, polymersomes, and other nanoparticles. In addition, ligands specific to the receptors overexpressed on cancer cells have been conjugated to these nanoparticles. Therefore, it is promising that delivering As[III] using nanotechnology would be applied as an anti-cancer drug option in treating a variety of solid cancers with improved efficacy and much less toxicity and it is essential to study the mechanisms by which cancer cells avoid apoptosis induced by As[III]. Autophagy, functioning synergistically with the KEAP1-NFE2L2 system, establishes a robust defense against metabolic and

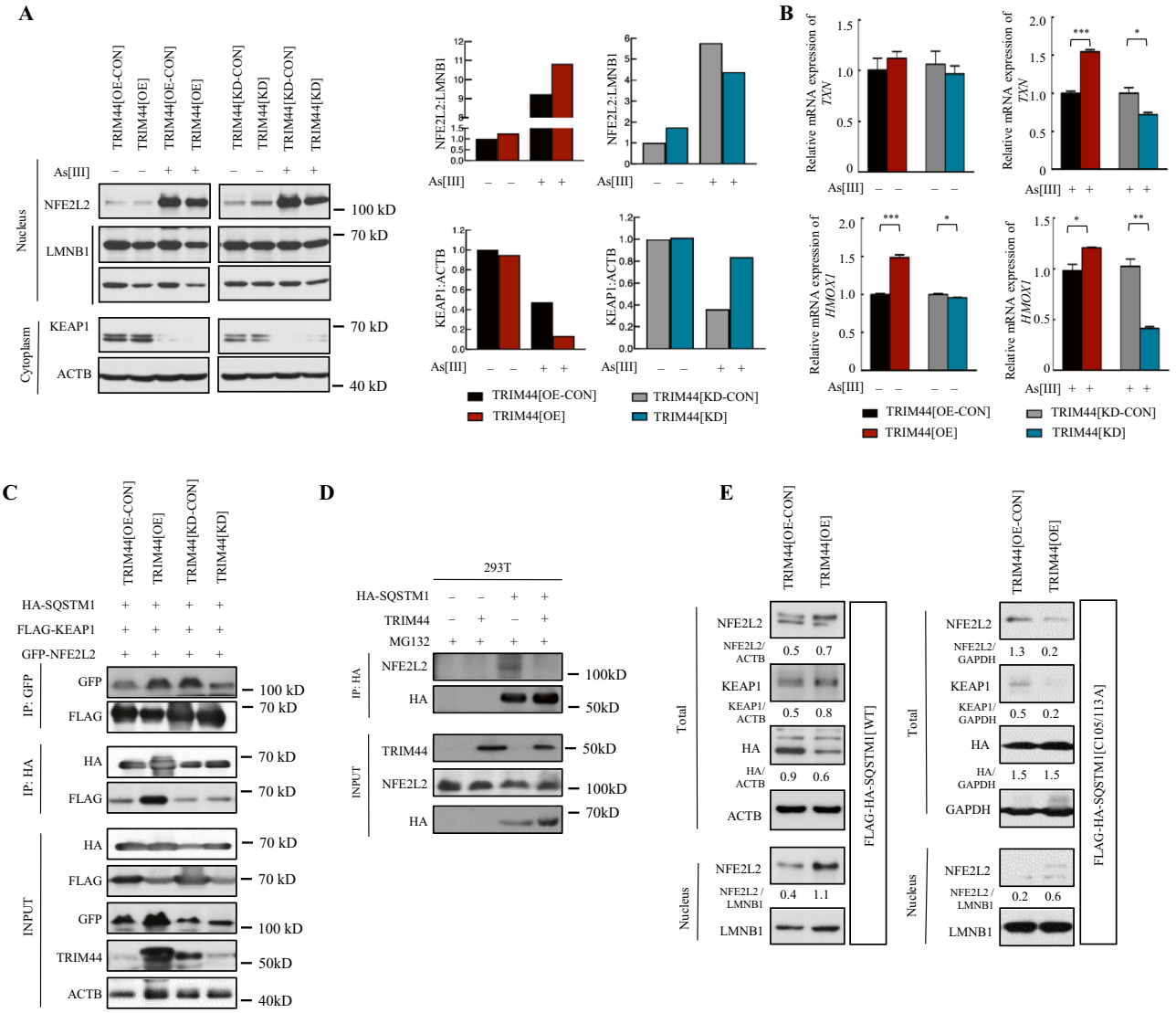


**Figure 7.** TRIM44 regulates the SQSTM1-KEAP1-NFE2L2 system. (**A**) U266 TRIM44[OE-CON], TRIM44[OE], TRIM44[KD-CON] and TRIM44[KD] cells were treated with or without As[III] (5 μM, 6 h). Nuclear fractions and cytoplasmic fractions were prepared and then subjected to immunoblot analysis with indicated antibodies. Relative levels of NFE2L2 in nuclear and KEAP1 in cytoplasm were quantified. (**B**) Quantitation of messenger RNA (mRNA) levels of NFE2L2 targets in U266 stable cells. Cells were challenged with or without As[III] (5 μM, 24 h) and then subjected to qRT-PCR analysis with indicated genes. The experiments were performed three times. Data are mean ± SD. Statistical analysis was carried out using Student's *t* test, with $^{*}P < 0.05$, $^{**}P < 0.01$ and $^{***}P < 0.001$. (**C**) Immunoprecipitation assays. 293T (TRIM44[OE-CON], TRIM44[OE], TRIM44[KDCON], and TRIM44[KD]) cells were tri-transfected with indicated plasmids. After 48 h, cells were subjected to immunoprecipitation with anti-GFP and anti-HA. Immunoblotting was performed with indicated antibodies. Data are representative of three independent experiments. (**D**) Immunoprecipitation assays. 293T cells were co-transfected with indicated plasmids. After 48 h, cells were treated with MG132 (5 μM) for 6 h and then subjected to immunoprecipitation with anti-HA. Immunoblotting was performed with indicated antibodies. Data are representative of three independent experiments. (**E**) Immunoblot analysis. 293T cells stably co-expressing FLAG-HA-SQSTM1 wild-type (WT) or its mutation (C105/113A) with TRIM44 (TRIM44[OE]) or without TRIM44 (TRIM44[OE-CON]) were treated with As[III] (5 μM, 6 h). Total cell lysates and nuclear fractions were prepared and analyzed by immunoblotting for indicated antibodies.

oxidative stresses. These two pathways are intricately connected, as demonstrated by the phosphorylation of the ubiquitin-binding autophagy receptor protein SQSTM1 with the SQSTM1–KEAP1–NFE2L2 pathway[38]. Our results showed that TRIM44 emerges as a crucial mediator in this interplay and promotes autophagy in response to As[III] induced oxidative stress which results in decreased cytotoxicity.

## Materials and methods

### Cell lines

HeLa, HEK293T, U266 cell lines were obtained from ATCC (Rockland, MD). We verified these cell lines via STR profiling (short tandem repeat analysis of DNA). Cell lines that contained knockout or overexpression constructs were not passaged beyond ~ 8 generations (1–1.5 months).

HeLa and HEK293T cells were cultured in in Dulbecco's Modified Eagle's medium (Corning, 10-013-CM) with 10% FBS (Peak serum, PS-FB1). U266 cells were cultured in RPMI medium (GE Healthcare Life Sciences, SH30255.01) with 10% FBS. We generated cells in which TRIM44 was overexpressed (TRIM44[OE]) or knocked down (TRIM44[KD]) via a lentivirus. Control cells were infected with relevant control vectors corresponding to the infecting virus vector (TRIM44[OE-CON] or TRIM44[KDCON]). Lentivirus were packaged using transfer vector (OHS5898-202620525, or RHS4430-200177847), viral packaging (psPAX2), and viral envelope (pMD2G) in 293FT cells.

### Antibodies

Anti-TRIM44 polyclonal antibody (Proteintech Group, 11511-1-AP); anti-Ub antibody (Biolegend, 646301); anti-mCherry antibody (ThermoFisher, PA5-34974); anti-NFE2L2 antibody (ThermoFisher, PA5-27882); anti-ATG5 antibody (Novus Biologicals, NBP224389); anti-GFP antibody (Santa Cruz Biotechnology, sc-9996); anti-ACTB antibody (Santa Cruz Biotechnology, sc-47778); anti-HA antibody (Santa Cruz Biotechnology, sc-805); anti-LC3B antibody (Cell Signaling Technology, 3868); anti-SQSTM1 antibody (Cell Signaling Technology, 88588); anti-LaminB1 antibody (R&D, MAB8525); antiKEAP1 antibody (Origene, TA502059); anti-GAPDH antibody (Invitrogen, PA5-85074); anti-FLAG antibody (Invitrogen, PA1-984); anti-mTOR antibody (CST, 2972); antiphospho-mTOR (Ser2448) antibody (Millipore Sigma, 09-213) anti-SQSTM1 antibody(CST, 7695,88588); anti-phospho-SQSTM1/p62 (Ser349) (E7M1A) antibody (CST, 16177S); anti-phospho-SQSTM1/p62 (Ser403) (D8D6T) antibody (CST, 39786S); anti-PKA Cα antibody (CST, 4782); anti-PKA substrate antibody (CST, 9624); Goat anti-Mouse IgG (Invitrogen, 31430); Goat anti-Rabbit IgG (Invitrogen, 31460); Alexa Fluor 594 donkey anti rabbit IgG (H + L) (Invitrogen, A21207); Alexa Fluor 546 goat anti mouse IgG (H + L) (Invitrogen, A11003).

### Reagents

MG132 (Selleck Chemicals, s2619); 3-Methyladenine (3-MA) (Selleck Chemicals, s2767); torkinib (PP242) (Selleck Chemicals, s2218); arsenic trioxide (As[III]) (SigmaAldrich, 01969); chloroquine (Sigma-Aldrich, C6628); bafilomycin A1 (MedChemExpress, HY-100558); rotenone (Sigma-Aldrich, 557368).

### Plasmids

To construct SQSTM1 truncates, a series of deletions of SQSTM1 were amplified by PCR using appropriate primers and cloned into the HA empty vector. GFP-TRIM44, and its deletion mutant expression plasmids have been described previously[24].

### Apoptosis assay

MM cells were irradiated with 5 μM As[III] and harvested after 24 h. The cells were stained with PE-Annexin V and 7-AAD (BD Bioscience, 559763) and examined with an LSR-II flow cytometer. The percentage of apoptosis was analyzed using FACS Diva software version 8.0.1 (BD Bioscience) (https://www.bdbiosciences.com/en-us/products/software/instrument-software/bd-facsdiva-software).

### Confocal microscopy

The cells were fixed with 4% paraformaldehyde (Thermo Fischer scientific, AAJ61899AK) and permeabilized with 0.2% triton-X 100 (Sigma-Aldrich, 93443). Following blocking with Animal-Free Blocker (Vector laboratories, SP-5030-250) for 1 h, followed by washing with 1× phosphate buffer saline (PBS) (Corning, 46-013-CM; pH 7.4). The cells were then incubated with indicated antibodies overnight at 4 °C, washed 3 times with PBS and incubated with fluorochrome-conjugated secondary antibodies for 1 h at room temperature, washed 3 times with PBS and incubated with DRAQ5 (Cell Signaling Technology, 4084) for 30 min. Slides were analyzed by confocal microscope Leica TCS SP5 and processed with the software LAS X Version 3.3.0 (Leica Microsystems) (https://www.leica-microsystems.com/products/microscope-software/p/leica-las-x-ls/). To quantify indicated protein levels, four or five random images were taken from each slide, and were quantified with ImageJ 1.53t software (National Institutes of Health) (https://imagej.net/ij/). To quantify cells with SQSTM1 aggregates, we counted the total number of cells in each image using the "Analyze Particles" from ImageJ. For the size parameter (pixel$^2$), we applied a range of 4000-Infinity to count the number of HeLa cells. To count cells with more than two visible SQSTM1 aggregates, we used the "Cell Counter" feature from ImageJ[21].

### Immunoprecipitation and immunoblotting

Cells were lysed in NP-40-containing lysis buffer (BP-119, Boston Bioproducts, Ashland, MA, USA) containing protease inhibitors mixture (11697498001, Complete; Roche Diagnostics, Mannheim, Germany) and phosphatases inhibitors and incubated with indicated antibodies together with the protein A/G plus-agarose immunoprecipitation reagent (Santa Cruz Biotechnology, sc-2003) at 4 °C overnight. Immunoprecipitates were eluted with Laemmli sample buffer (Bio-Rad) and analyzed using the indicated antibodies.

### CHX chase assay
MM cells were seeded into 6-well plates at a density of $3 \times 10^5$ cells/well and incubated overnight at 37 °C in a CO2 incubator. Cells were treated with 50 μg/ml of CHX dissolved in absolute ethanol, and harvested in ice cold phosphate buffered saline (PBS, pH 7.4) at varying chase points by centrifugation at 2500 × g for 10 min at 4 °C. Cell pellets were lysed in a lysis buffer. Samples were heated at 95 °C for 10 min.

### Cell lysate fraction
Cells were lysed in a NP-40-containing lysis supplemented with protease inhibitors mixture and centrifuged at 15,000 × g into supernatant (Non-aggregates) and pellet (Aggregates) fractions. Both fractions were boiled in buffer containing 1% SDS and analyzed by western blot.

### DSP crosslinking
Cells with less than 80% confluence were washed twice with ice-cold washing puffer ($Na_2HPO_4$ 10 mM, $KH_2PO_4$ 1.8 mM, NaCl 137 mM, KCl 2.7 mM, $CaCl_2$ 0.1 mM, and $MgCl_2$ 1 mM). They were then incubated in the washing buffer with 0.4 mg/ml DSP at 4 °C for 2 hours. Afterward, the cells were lysed in IP lysis buffer containing 1% SDS and sonicated for 10 seconds. Following sonication, the lysate was diluted with IP lysis buffer at a 1:10 ratio and subjected to immunoprecipitation[28].

### Cell transfection
Cells were transfected by Lipofectamine™ 3000 tansfection reagent (Invitrogen, L3000015) following the protocol.

### Nuclear fraction extraction
Nuclear fractions were extracted by kit (Active Motif, 40010).

### Statistical analysis
Statistical analysis was conducted using GraphPad Prism 10 software (https://www.graphpad.com/scientific-software/prism/). Differences among groups were determined using one-way analysis of variance (ANOVA) followed by Tukey's multiple comparison test. A $p$ value of less than 0.05 was considered statistically significant. All values in the results are expressed as means ± SD, based on at least 3–5 independent experiments.

## Data availability
The data that support the findings of this study are available on request from the corresponding author upon reasonable request.

Received: 19 March 2024; Accepted: 16 July 2024
Published online: 16 August 2024

## References
1. Aman, Y. *et al.* Autophagy in healthy aging and disease. *Nat. Aging* **1**(8), 634–650 (2021).
2. Cui, H., Kong, Y. & Zhang, H. Oxidative stress, mitochondrial dysfunction, and aging. *J. Signal Transduct.* **2012**, 646354 (2012).
3. Finkel, T. & Holbrook, N. J. Oxidants, oxidative stress and the biology of ageing. *Nature* **408**(6809), 239–247 (2000).
4. Hayes, J. D., Dinkova-Kostova, A. T. & Tew, K. D. Oxidative stress in cancer. *Cancer Cell* **38**(2), 167–197 (2020).
5. Lin, M. T. & Beal, M. F. Mitochondrial dysfunction and oxidative stress in neurodegenerative diseases. *Nature* **443**(7113), 787–795 (2006).
6. Anding, A. L. & Baehrecke, E. H. Cleaning house: Selective autophagy of organelles. *Dev. Cell* **41**(1), 10–22 (2017).
7. Murrow, L. & Debnath, J. Autophagy as a stress-response and quality-control mechanism: Implications for cell injury and human disease. *Annu. Rev. Pathol.* **8**, 105–137 (2013).
8. Shen, Z. X. *et al.* Use of arsenic trioxide ($As_2O3$) in the treatment of acute promyelocytic leukemia (APL): II. Clinical efficacy and pharmacokinetics in relapsed patients. *Blood* **89**(9), 3354–3360 (1997).
9. Akhtar, A. *et al.* Recent advances in arsenic trioxide encapsulated nanoparticles as drug delivery agents to solid cancers. *J. Biomed. Res.* **31**(3), 177–188 (2017).
10. Mizushima, N. *et al.* Autophagy fights disease through cellular self-digestion. *Nature* **451**(7182), 1069–1075 (2008).
11. Bellezza, I. *et al.* Nrf2-Keap1 signaling in oxidative and reductive stress. *Biochim. Biophys. Acta Mol. Cell Res.* **1865**(5), 721–733 (2018).
12. Komatsu, M. *et al.* The selective autophagy substrate p62 activates the stress responsive transcription factor Nrf2 through inactivation of Keap1. *Nat. Cell Biol.* **12**(3), 213–223 (2010).
13. Lau, A. *et al.* A noncanonical mechanism of Nrf2 activation by autophagy deficiency: Direct interaction between Keap1 and p62. *Mol. Cell Biol.* **30**(13), 3275–3285 (2010).
14. Watanabe, M. & Hatakeyama, S. TRIM proteins and diseases. *J. Biochem.* **161**(2), 135–144 (2017).
15. Allen, M. D. & Bycroft, M. The solution structure of the ZnF UBP domain of USP33/VDU1. *Protein Sci.* **16**(9), 2072–2075 (2007).
16. Boutou, E., Matsas, R. & Mamalaki, A. Isolation of a mouse brain cDNA expressed in developing neuroblasts and mature neurons. *Mol. Brain Res.* **86**(1–2), 153–167 (2001).
17. Kawaguchi, T. *et al.* Overexpression of TRIM44 is related to invasive potential and malignant outcomes in esophageal squamous cell carcinoma. *Tumour Biol.* **39**(6), 1010428317700409 (2017).
18. Liu, S. *et al.* Overexpression of TRIM44 is an independent marker for predicting poor prognosis in epithelial ovarian cancer. *Exp. Ther. Med.* **16**(4), 3034–3040 (2018).
19. Yamada, Y. *et al.* A novel prognostic factor TRIM44 promotes cell proliferation and migration, and inhibits apoptosis in testicular germ cell tumor. *Cancer Sci.* **108**(1), 32–41 (2017).
20. Zhu, X. *et al.* High expression of TRIM44 is associated with enhanced cell proliferation, migration, invasion, and resistance to doxorubicin in hepatocellular carcinoma. *Tumour Biol.* **37**(11), 14615–14628 (2016).

21. Lyu, L., Chen, Z. & McCarty, N. TRIM44 links the UPS to SQSTM1/p62-dependent aggrephagy and removing misfolded proteins. *Autophagy* **18**(4), 783–798 (2022).
22. Levy, J. M. M., Towers, C. G. & Thorburn, A. Targeting autophagy in cancer. *Nat. Rev. Cancer* **17**(9), 528–542 (2017).
23. Lyu, L., Lin, T. C. & McCarty, N. TRIM44 mediated p62 deubiquitination enhances DNA damage repair by increasing nuclear FLNA and 53BP1 expression. *Oncogene* **40**(32), 5116–5130 (2021).
24. Chen, Z. *et al.* TRIM44 promotes quiescent multiple myeloma cell occupancy and survival in the osteoblastic niche via HIF-1α stabilization. *Leukemia* **33**(2), 469–486 (2019).
25. Yang, B. *et al.* Novel function of Trim44 promotes an antiviral response by stabilizing VISA. *J. Immunol.* **190**(7), 3613–3619 (2013).
26. Bjørkøy, G. *et al.* p62/SQSTM1 forms protein aggregates degraded by autophagy and has a protective effect on huntingtin-induced cell death. *J. Cell Biol.* **171**(4), 603–614 (2005).
27. Jakobi, A. J. *et al.* Structural basis of p62/SQSTM1 helical filaments and their role in cellular cargo uptake. *Nat. Commun.* **11**(1), 440 (2020).
28. Pan, J. A. *et al.* TRIM21 ubiquitylates SQSTM1/p62 and suppresses protein sequestration to regulate redox homeostasis. *Mol. Cell* **61**(5), 720–733 (2016).
29. Ciuffa, R. *et al.* The selective autophagy receptor p62 forms a flexible filamentous helical scaffold. *Cell Rep.* **11**(5), 748–758 (2015).
30. Carroll, B. *et al.* Oxidation of SQSTM1/p62 mediates the link between redox state and protein homeostasis. *Nat. Commun.* **9**(1), 256 (2018).
31. Fass, E. *et al.* Microtubules support production of starvation-induced autophagosomes but not their targeting and fusion with lysosomes. *J. Biol. Chem.* **281**(47), 36303–36316 (2006).
32. Li, N. *et al.* Mitochondrial complex I inhibitor rotenone induces apoptosis through enhancing mitochondrial reactive oxygen species production. *J. Biol. Chem.* **278**(10), 8516–8525 (2003).
33. Ichimura, Y. *et al.* Phosphorylation of p62 activates the Keap1-Nrf2 pathway during selective autophagy. *Mol. Cell* **51**(5), 618–631 (2013).
34. Lim, J. *et al.* Proteotoxic stress induces phosphorylation of p62/SQSTM1 by ULK1 to regulate selective autophagic clearance of protein aggregates. *PLoS Genet.* **11**(2), e1004987 (2015).
35. Matsumoto, G. *et al.* Serine 403 phosphorylation of p62/SQSTM1 regulates selective autophagic clearance of ubiquitinated proteins. *Mol. Cell* **44**(2), 279–289 (2011).
36. Katsuragi, Y., Ichimura, Y. & Komatsu, M. p62/SQSTM1 functions as a signaling hub and an autophagy adaptor. *FEBS J.* **282**(24), 4672–4678 (2015).
37. Taguchi, K. *et al.* Keap1 degradation by autophagy for the maintenance of redox homeostasis. *Proc. Natl. Acad. Sci. U. S. A.* **109**(34), 13561–13566 (2012).
38. Ichimura, Y. & Komatsu, M. Activation of p62/SQSTM1-Keap1-nuclear factor erythroid 2-related factor 2 pathway in cancer. *Front. Oncol.* **8**, 210 (2018).
39. Kao, S. H. *et al.* Analysis of protein stability by the cycloheximide chase assay. *Bio Protoc.* https://doi.org/10.21769/BioProtoc.1374 (2015).
40. Janasik, B. *et al.* Effect of arsenic exposure on NRF2-KEAP1 pathway and epigenetic modification. *Biol. Trace Elem. Res.* **185**(1), 11–19 (2018).
41. Baird, L. & Yamamoto, M. The molecular mechanisms regulating the KEAP1-NRF2 pathway. *Mol. Cell Biol.* https://doi.org/10.1128/MCB.00099-20 (2020).
42. Itakura, E. & Mizushima, N. p62 Targeting to the autophagosome formation site requires self-oligomerization but not LC3 binding. *J. Cell Biol.* **192**(1), 17–27 (2011).
43. Lamark, T. *et al.* Interaction codes within the family of mammalian Phox and Bem1p domain-containing proteins. *J. Biol. Chem.* **278**(36), 34568–34581 (2003).
44. Wilson, M. I. *et al.* PB1 domain-mediated heterodimerization in NADPH oxidase and signaling complexes of atypical protein kinase C with Par6 and p62. *Mol. Cell* **12**(1), 39–50 (2003).
45. Ikeda, R. *et al.* Phosphorylation of phase-separated p62 bodies by ULK1 activates a redox-independent stress response. *EMBO J.* **42**(14), e113349 (2023).


## Acknowledgements

We thank Dr. Viktor Korolchuk (Newcastle University, United Kingdom) for kindly providing us with the pLENTI6-V5-DEST-FLAG p62 Cys105A, 113A plasmids. This work was supported by a grant from the National Cancer Institute (NCI, CA181319).

## Author contributions

Y.W. and L.L. designed and performed the experiments. N.M. conceived the initial strategy and designed and supervised the work. Y.W., L.L., T.V., and N.M. wrote the manuscript. All authors reviewed the manuscript.

## Competing interests

The authors declare no competing interests.

## Additional information

**Supplementary Information** The online version contains supplementary material available at https://doi.org/10.1038/s41598-024-67832-x.

**Correspondence** and requests for materials should be addressed to N.M.